

Simulation of Physical Processes in Environmental Geology Laboratories

Dennis Hodge, Marcus Bursik, and David Barclay
Department of Geology
SUNY at Buffalo
Buffalo, New York 14260

ABSTRACT

The objective of our new introductory geology/environmental laboratories is to bring science to the students through computer-aided participatory laboratories. Field and laboratory data acquisition, statistical analysis and computer modeling of complex systems, are elements throughout the sequence of laboratories. Non-science students and introductory-geology students learn to develop multiple hypotheses, to understand the variability of data, to use computers for visualization of geologic phenomena, and to understand the importance of hypothesis testing as a societal responsibility.

The topics of the laboratories include earthquakes, mass wasting, volcanoes, topography, surface water chemistry and earth resources and materials. Although the topics are standard for introductory geology and environmental science, the approach described involves the use of interactive educational modules to learn the principles of a physical system. Laboratories on earthquakes, mass wasting, and volcanoes demonstrate how students use numerical experiments and graphical displays to study the interaction of variables in a physical system.

Keywords: Apparatus; education – geoscience; education – undergraduate; engineering and environmental geology; miscellaneous and mathematical geology.

INTRODUCTION

Traditionally, introductory geology courses have been a major attraction for the non-science student and the typical educational format in these courses has been the lecture and weekly laboratory session. Most of the laboratory manuals follow a standard topic format using content that has been used for almost 100 years. With the rapid change in computer accessibility and with the understanding that new informational technology is going to change the way students learn, we have developed a set of laboratories for students to learn physical geology using computer-aided techniques. These laboratory modules focus on environmental problems but the laboratories can serve students in introductory geology classes equally well.

Our approach is to teach a physical concept by using the computer to do numerical experiments and then to display the results in dynamic two and three-dimensional graphical illustrations. Because of the advances in computer speed, both in terms of numerical

calculations as well as graphical display, it is now possible to perform numerical “experiments” in beginning laboratory classes. We can incorporate complexities, thus allowing students to participate either directly in problem solving by manipulating variables, or, at the lower levels, to actually see, through demonstrations, the effects of such manipulations. The instruction system makes use of Macintosh computers which have real time three-dimensional graphics capabilities. This provides dramatic involvement of the student as she/he can see the effects of changes in the parameters of the physical system.

COMPUTER MODELS OF PHYSICAL PRINCIPLES

The laboratory topics include earthquakes, Earth's seismic structure, mass wasting, volcanoes, rivers, groundwater, topography, remote sensing, surface-water chemistry and earth resources and materials. Simple models of physical principles, often stated by a mathematical equation, are incorporated into every computer-aided laboratory and taught to the students through numerical experiments with the equation variables to show the response of the physical system (see Figure 1). These interactive computer modules are contained on CD-ROMs. An important element is that the students are learning by doing the exercises at their own pace.

To illustrate the concepts and elements of the interactive computer windows we have selected three examples from laboratories on earthquakes, mass wasting and volcanoes. These examples form only part of the entire sequence of interactive computer elements within the laboratories.

Earthquakes and Seismic Properties of the Earth's Interior

To understand the physical principles of propagation of seismic waves in the earth the students use an interactive computer program to learn Snell's Law, other refraction and reflection principles in the earth, and raypath geometry of seismic waves.

The first section of the laboratory is an instructional module in which the following types of illustrations are provided:

- still photographs of earthquake damage,
- animation of kinetic features, that is, the movement sense for a normal fault,
- video and audio short segments of earthquake phenomena
- instructional illustrations and diagrams,
- interactive exercises to learn seismic principles.

Elements of interactive laboratory modules

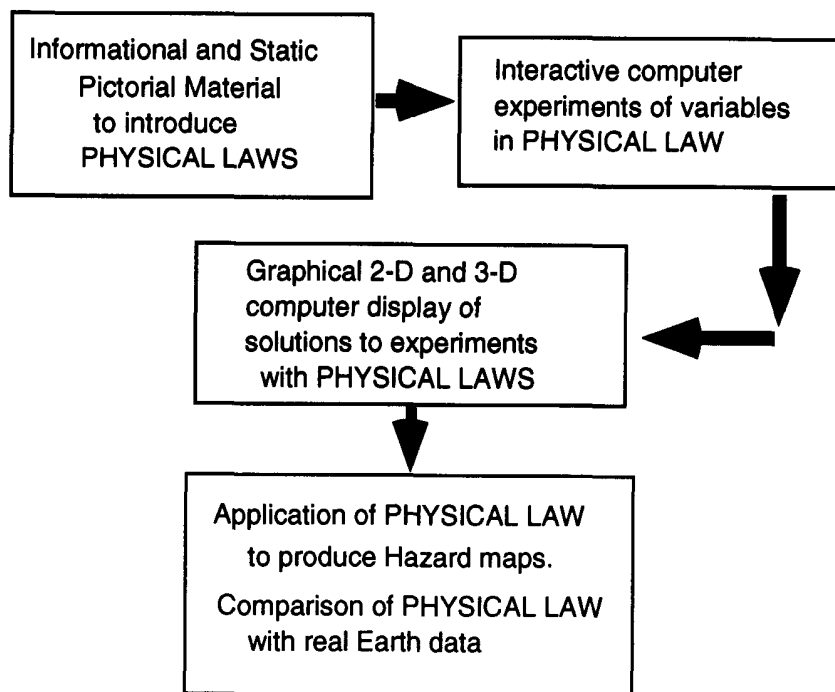


Figure 1. Schematic of interactive module design for study of physical laws.

Through lectures in the classroom and introductory books, the beginning student knows that in the interior of Earth there are large changes in the seismic velocities at boundaries such as the crust/mantle, the mantle/outer core, and the outer core/inner core. In the upper mantle, seismic velocity increases from a low-velocity region through the upper-mantle transition zone where velocities show several zones of markedly high rates of increase with depth. Below the transition zone seismic velocities show a gradual steady rise to the core. Seismic velocities have a circumferential homogeneous pattern in contrast to the significant vertical change of velocity with depth. In the laboratory we study the principles of seismic-wave refraction and how the vertical velocity structure in Earth dictates the raypaths of waves in the interior.

Graphical Experiments with Snell's Law

At a boundary in Earth separating layers of different seismic properties, some of the seismic energy is passed through the interface and changes direction. This is called refraction of seismic waves. A simple geometric relationship governs the angle of the incoming incident raypath to the angle of the refracted raypath. Consider two different rock types separated by a horizontal interface. If a seismic wave passes through the upper layer (layer 1) with a direction shown by the raypath in Figure 2, the direction of the seismic wave changes at the interface. The angle of the incident wave and the angle of the refracted

wave are related by the following equation:

$$\frac{\sin a}{V_1} = \frac{\sin b}{V_2} \quad (1)$$

where a and b are the incident angle and the refracted angle, respectively. These relationships are shown in Figure 2 where the velocities of the P-wave in the layers are V_1 and V_2 . This relationship is known as *Snell's law*.

The numerical experiments with graphical representation include variation of the angular relationship of seismic raypath and the seismic velocities of the media (see Figure 2). The principles of seismic refraction are investigated using a simple horizontal two-layer case. In the initial numerical experiment the upper layer has a lower velocity than the lower layer (V_2 is greater than V_1). After selection of a number of velocity combinations for the two layers, the students reach the conclusion that if the velocity in the lower layer, V_2 , is greater than V_1 , the angle of refraction (b) will

be larger than the incident angle (a). The graphical representation enhances the simple conclusion denoted by equation 1.

Raypath Geometry in Mantle and Shadow Zone

The raypaths of seismic body waves in the mantle are continuously refracted as they propagate downward, ultimately being refracted back to the surface. The raypath is roughly a segment of a circle for a P-wave that travels through the mantle. Seismologists also noticed that beyond a distance of 103 degrees, the P and S waves do not arrive at the expected time. Indeed seismologists noted that the S-wave is not recorded beyond this arc distance and the P-wave is not recorded between a distance of 103 and 142 degrees. These are the questions posed to the students for numerical experimentation.

To illustrate how increasing seismic velocities in the mantle affect the raypath of body waves, we make several simplifying assumptions; 1) the mantle is composed of a number of concentric shells or layers with constant velocity and 2) each successively deeper layer (shell) has a higher velocity of transmission of seismic body waves (Figure 3). In this example P waves are refracted at each boundary of the concentric shells. For a downgoing wave the incident angle at a boundary will be smaller than the refracted angle. Calculation of the P-wave refraction angles successively downward in this 'layered' mantle and the plot of the raypath of the waves shows a roughly circular raypath in the mantle.

Seismic Waves - Earth's Interior

Snell Exercise

Set the velocity for each of the two layers.

Layer 1:

Layer 2:

Find the critical angle based on your velocity settings for the two layers.

Click on the vector and drag it to the right to see the results of Snell's law at that angle of incidence.

Snell's law:

$$\frac{\sin a}{V_1} = \frac{\sin b}{V_2}$$

$$\frac{\sin 52.4}{1400} = \frac{\sin 26.9}{8000}$$

The critical angle is at:

$$\sin i_c = \frac{V_1}{V_2}$$

Set Velocities

The diagram shows a horizontal boundary between Layer 1 (velocity 14000) and Layer 2 (velocity 8000). An 'Energy Source' is located in Layer 1. A ray originates from the source and travels towards the boundary. At point 'a' on the boundary, the ray is incident at an angle 'a' to the normal. It refracts into Layer 2 at point 'b' at an angle 'b' to the normal. A third ray is shown incident at the critical angle 'c' to the normal, which travels along the boundary between the two layers.

Figure 2. Interactive computer window teaching Snell's Law. This and all other computer windows have been simplified from the originals for presentation in paper format.

In a second part of the exercise the cause of the shadow zone is determined. P-waves dive through the mantle and if they intersect the boundary between the mantle and the liquid outer core, the seismic waves are refracted. The velocity of propagation of P-waves in the outer core is about 8.0 km/s, much less than the seismic velocity of about 14 km/s in the lower-most mantle. Under these conditions and using Snell's Law of refraction, it is obvious that the angle of refraction will be smaller than the angle of incidence. The incident P-wave traveling in the lower mantle will be refracted away from the mantle/core boundary. A P-wave that just passes above the mantle/core boundary is recorded at Earth's surface at a distance of 103° from the source. A P-wave that has a raypath slightly deeper intersects the mantle/core boundary and is deflected into the core and ultimately arrives at Earth's surface at a distance of 142° from the source. This phenomenon causes the shadow zone at the Earth's surface. Using the Snell's Law interactive window students choose the appropriate velocity of the lower mantle and the outer core from Figure 3B and note the angular relationships of

P-waves that intersect the outer core/mantle boundaries at a series of angles. The trajectory of the P-waves refracted into the outer core from the mantle/core boundary are plotted and the explanation for the shadow zone is graphically illustrated.

MASS WASTING AND LANDSLIDE HAZARDS

In the *Mass Wasting and Landslide Hazards* laboratory, students first read a narrative section illustrating different mass-wasting processes and concepts such as the angle of repose. Next the students use an interactive model to learn the relative importance of factors affecting stability of a rotational slump. The final section of the laboratory teaches spatial aspects of landslide hazards.

Factors Affecting Slope Stability: The Interactive Rotational Slump Model

This section of the laboratory teaches students the relative importance of different factors affecting slope stability using an interactive model of a rotational slump. In a graphic interface showing the profile of the slump (Figure 4), students can alter the slope geometry

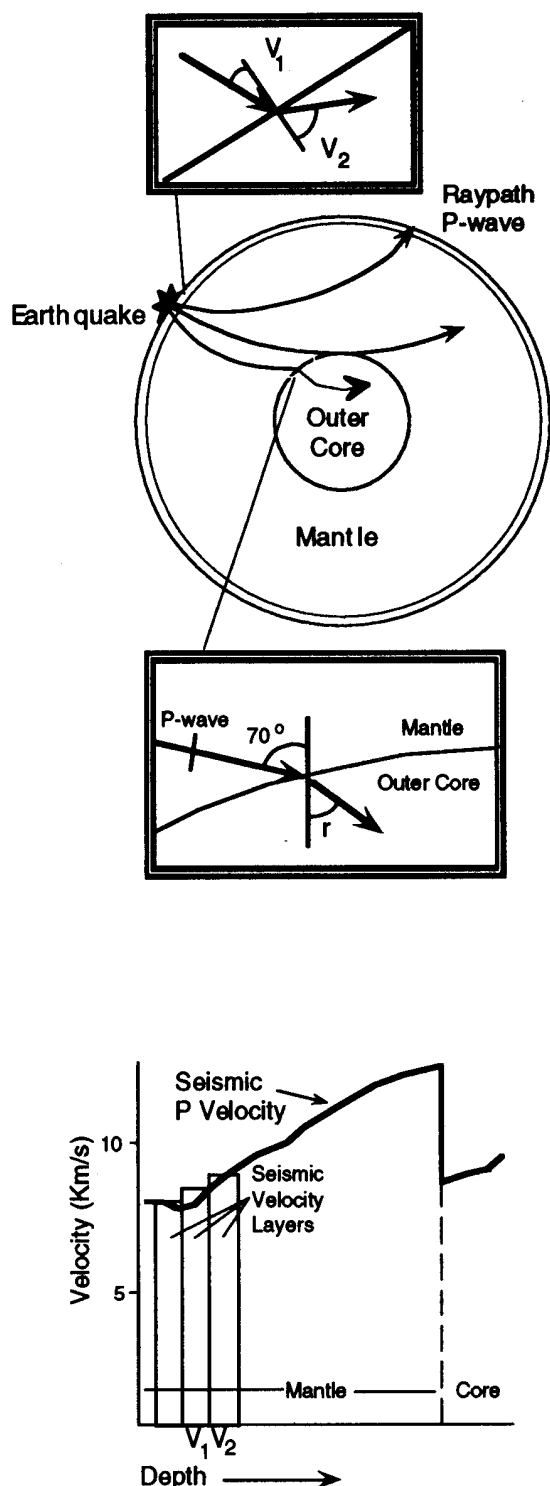


Figure 3. A. Raypath geometry of P-waves in Earth's mantle. Mantle subdivided into discrete constant velocity layers. B. P-wave velocity distribution in mantle and core with discrete velocity layers shown.

and level of the water table while physical properties of the soil are selected from a menu.

The model uses the Method of Slices to simulate the slump with the Factor of Safety determined as:

$$F = \frac{\sum \{c' + (W \cos \alpha - \mu l) \tan \phi'\}}{\sum W \sin \alpha} \quad (2)$$

In this equation cohesion (c') and the angle of internal friction (ϕ') are chosen from the menu of soil properties while the failure surface length (l), the weight of the soil above the failure surface (W), the angle of the failure surface from horizontal (α) and the porewater pressure at the failure surface (μ) are determined for each slice by the computer from the graphic interface. Students observe and interpret their manipulations of the model using general forms of the equations describing the Factor of Safety and moments of the forces driving and resisting motion:

$$FS = M_r / M_d, \quad (3)$$

$$M_d = W A, \text{ and} \quad (4)$$

$$M_r = L S R, \quad (5)$$

where FS is the Factor of Safety, M_d and M_r are the moments of the forces driving and resisting motion, W the weight of soil above the failure surface, A the length of the lever arm, L the length of the failure surface, S the shear strength of the soil, and R the radius of the failure circle.

The equations are recalculated to general forms for display to reduce the complexity of the mathematics that may obscure the information being passed on to the student.

Students are guided through an exercise in which they remove material from the base of the slope and add material to the top. This represents undercutting of the slope by, for example, river erosion or road building, and dumping of soil, for example, during mining operations. Students also compare the slope stability of steep versus shallow slope profiles and high versus low water tables. For each modification the students make to the slope geometry, water table position, or soil parameters, the screen displays equations 3, 4, and 5 and prompts the student to interpret what they have done. By considering how the variables and the Factor of Safety change, students learn how progressive changes to slope geometry, through both natural processes and human activities, can lead to a slope becoming more unstable. Use of this interactive model also shows how water acts as the trigger in slope failure events. This important role of water is expanded upon in a follow-up tutorial section which uses Coulomb's Law to show how changes in water content of the soil affect the shear strength.

Spatial Aspects of Landslide Hazards

The final section of this laboratory teaches spatial aspects of landslide hazards. Whereas fluctuations in the water content of the soil determine when a slope may fail, the location of soil types susceptible to failure and steep slopes determines where a landslide will occur. The exercise is based on a landslide hazard

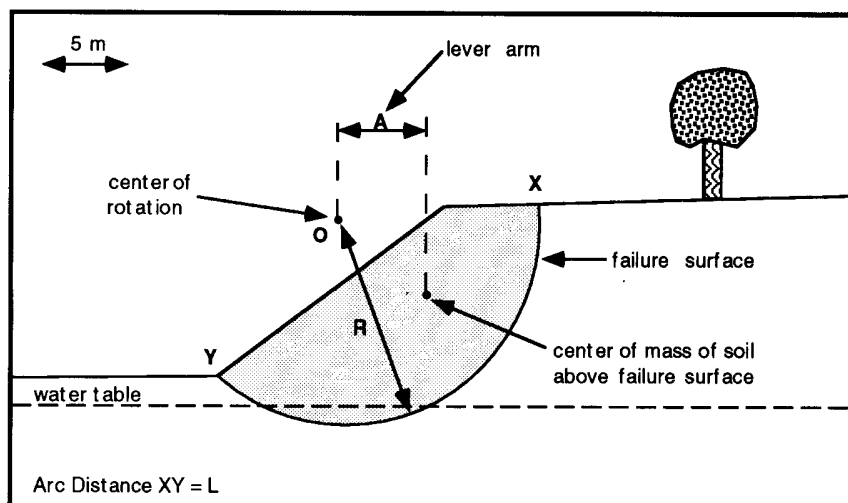


Figure 4. Interactive rotational slump model.

analysis study in the Tully Valley region, New York, by Jager and Wieczorek (1994) and uses a composite-mapping technique to combine different factors affecting slope stability into a hazard map (Figure 5).

The locations of historic and prehistoric landslides in the Tully Valley region correlate to three factors that can be represented on maps: slope steepness, agricultural soil types and locations of glacial lakes at the end of the last glaciation. Students are given maps of these three factors with grid overlays and are required to assign hazard parameter values to each cell (Table 1). The hazard parameter is a number that expresses the relative risk of landsliding for each classification of slope steepness, agricultural soil type, and glacial-lake level. Higher values represent higher hazard. This section of the laboratory teaches students how a "vector"-style map can be converted to a digital "raster"-style map where space is represented as cells in a grid. Students are also required to make important judgments concerning how they apply the hazard parameters to cells. For example, a cell is 40% "clay" agricultural soil type (hazard parameter = 0.7) and 60% "non-clay" agricultural soil type (hazard parameter = 0.3). Should the student assign the cell a hazard parameter value of 0.3 because "non-clay" forms the majority of the cell, a value of 0.7 to err on the side of safety, or split the difference and assign a value of 0.5? This makes students consider bias in interpreting data and how this can affect the resulting prediction of the location of landslide hazards.

The hazard map is completed by adding the hazard parameters from the maps of the three factors for each cell and entering the total onto a composite map. The level of hazard is classified as in Table 2 and the students shade their composite map accordingly. Maps showing roads and settlements are then provided and students write a concluding statement in which they interpret the location and relative hazard

of landslides in the region. To increase the area covered in the hazard analysis students can individually complete the computations for different sectors of the region and then use results from the whole class in the final interpretation.

VOLCANIC-FLOW PHENOMENA AND ESTIMATION OF VOLCANIC HAZARDS

In their exploration of volcanic-flow phenomena and volcanic hazards, the students are first taken through a tutorial of informational material. This material introduces students to the concepts that they will be exploring in the module on volcanic eruptions. As they are exploring volcanic eruptive processes, they are shown the

causes of eruptions with a concentration on the degassing of magma, typical products (especially the different types of lava and their physical properties), and eruptive phenomena. The eruptive phenomena they will explore further in the computer module are lava flows, nuees ardentes, and lahars.

Lava flows, nuees ardentes, and lahars are all ground-hugging flows. In the next section of the module, students perform numerical experiments with these different types of flows from a custom-built window (Figure 6). The window shows the equations to be used in words and the mathematical symbols. The equations are the typical equations for fluid flow, continuity:

$$\nabla \cdot \rho \mathbf{v} = 0,$$

which for the numerical operations is simplified to:

$$v_i D_i = v_0;$$

and the Navier-Stokes equation:

$$\rho \frac{\partial \mathbf{v}}{\partial \tau} = -\nabla P + \kappa \nabla^2 \mathbf{v} + \rho \mathbf{g},$$

which can be written in integral form as:

$$\rho' D \frac{\partial v}{\partial \tau} = -\frac{v}{D} v - \frac{1}{2} C_D \rho' v^2 + \rho' D g \sin \theta,$$

and finally solved numerically from the simplified equation:

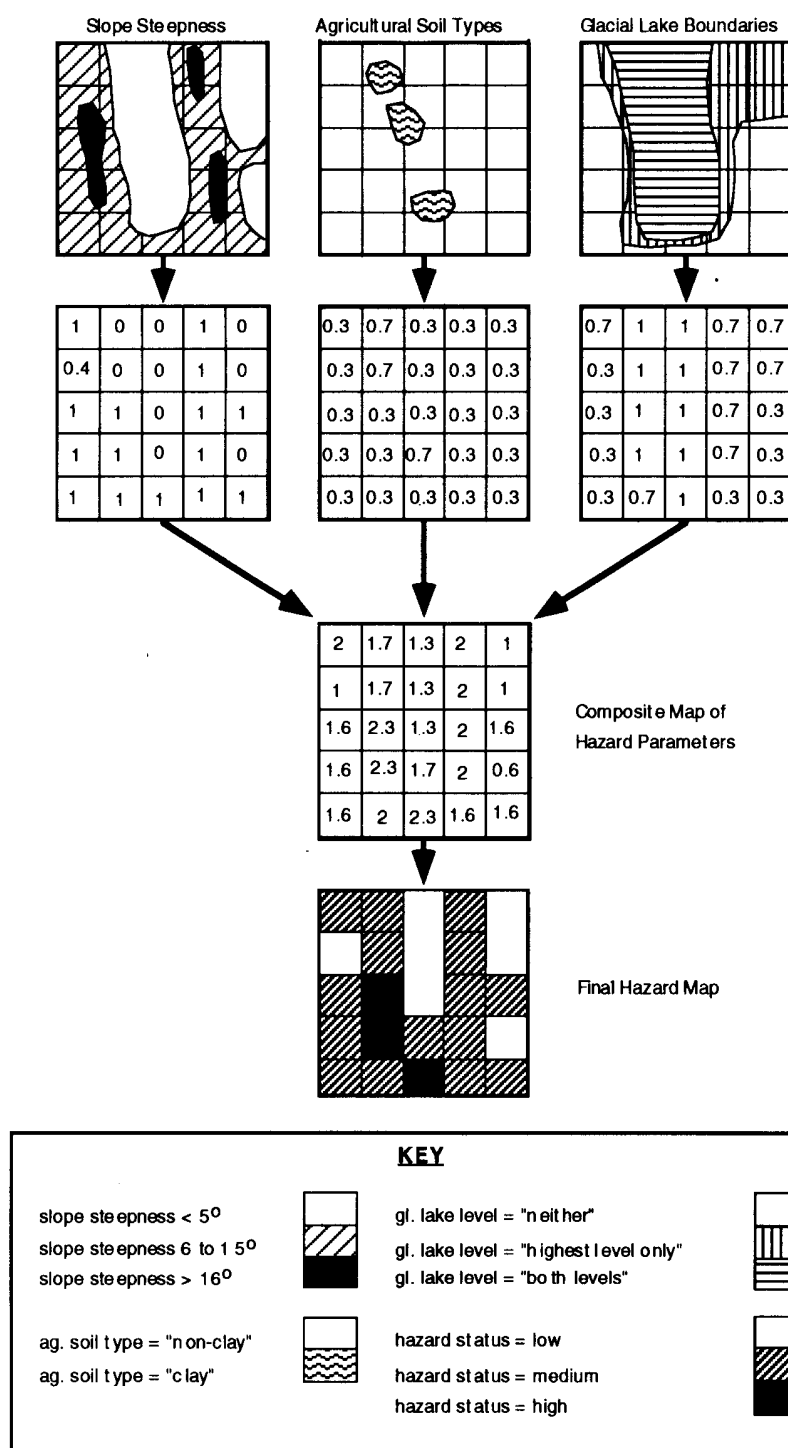


Figure 5. Composite mapping technique applied to landsliding hazard.

$$\nabla v_{i+1} = \left[g \sin \vartheta - \frac{\alpha v_i + \beta v_i^2}{\rho' D} \right] \Delta \tau,$$

where v_i is the downslope velocity of the flow in time step i , g is acceleration due to gravity, κ and ν are respectively dynamic and kinematic viscosity, C_D is a

some "edge" of the integration space) and constant parameters. To limit their choices so that they are not overwhelmed, however, we have found it best to allow the students to vary only some of these (Figure 6). If the students are allowed to vary only ϑ , β and α , ρ and D_0 , they will be able to study the effects of changing slope angle, bed friction, air resistance, initial density contrast and initial thickness.

Variable	Hazard Parameter Value
slope steepness <5°	0
slope steepness 6 to 15°	1.0
slope steepness >16°	0.4
ag. soil = non-clay	0.3
ag. soil = clay	0.7
gl. lake = neither	0.3
gl. lake = highest level only	0.7
gl. lake = both levels	1.0

Table 1

Hazard Status	Hazard Parameter Range
low	<1.31
medium	1.31 to 2.26
high	>2.26

Table 2

drag coefficient, ϑ is slope angle, α and β are empirical constants dependent on flow viscosity and air resistance respectively, ρ is flow density, ρ' is flow density, ρ is $\rho' - \rho_0/\rho$, D is flow thickness, and τ is time. Hence in any time step, the flow will have velocity:

$$v_i = v_{i-1} + \Delta v_i,$$

and thickness:

$$D_i = \frac{v_0 D_0}{v_i}.$$

This model represents a considerable simplification of reality, but we have found it to yield solutions that are reasonable when truncated at some finite velocity. In theory, students could study the effects of changing all boundary conditions (the values of the variables at

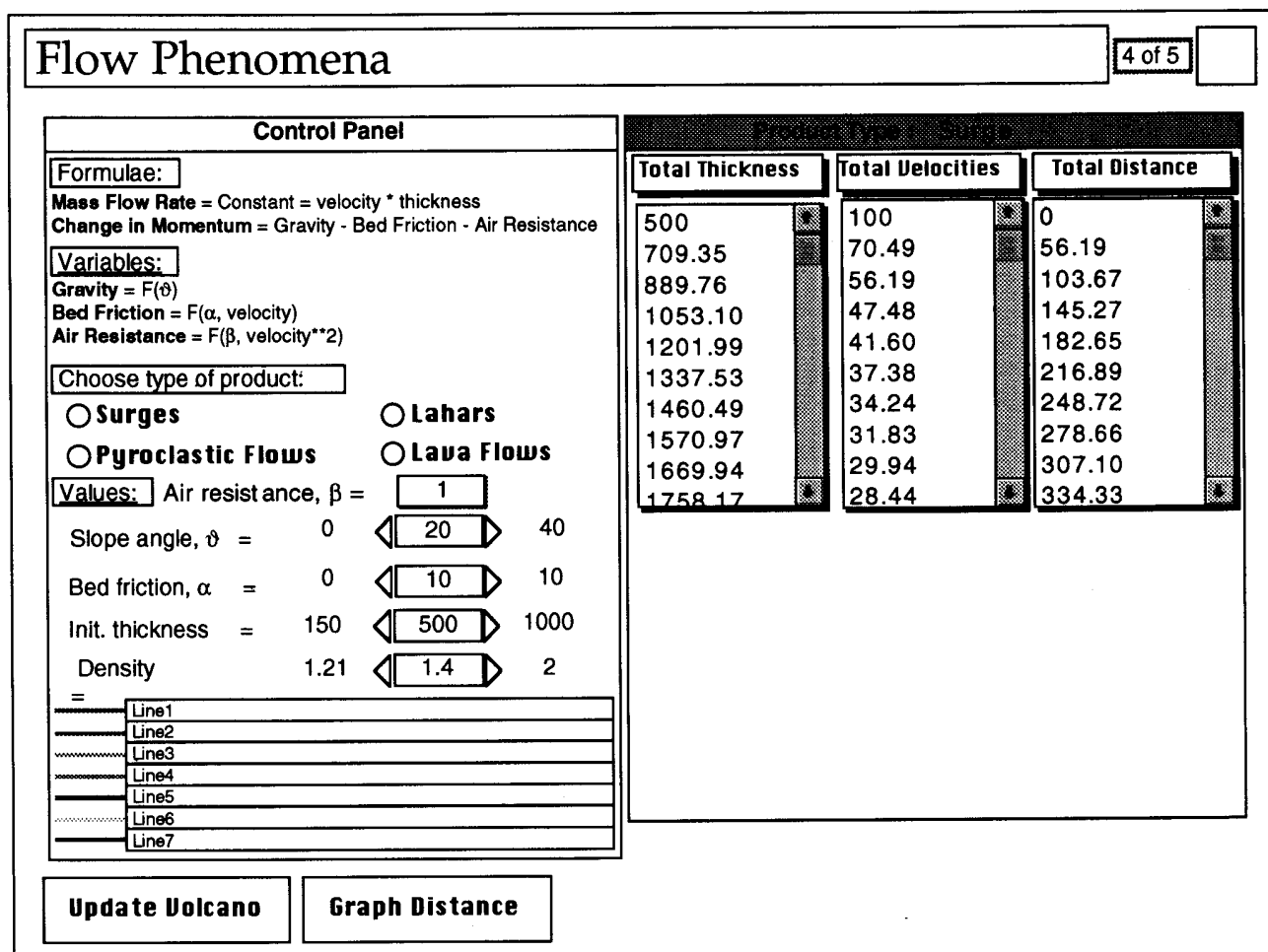


Figure 6. The graphical user interface (GUI) window for the volcano numerical experiments shows the equations (in words) and variable dependencies. Students adjust the parameter values, and after clicking on 'Update Volcano' are shown the values for velocity, thickness, and distance traveled as functions of time. These results can be plotted (not shown).

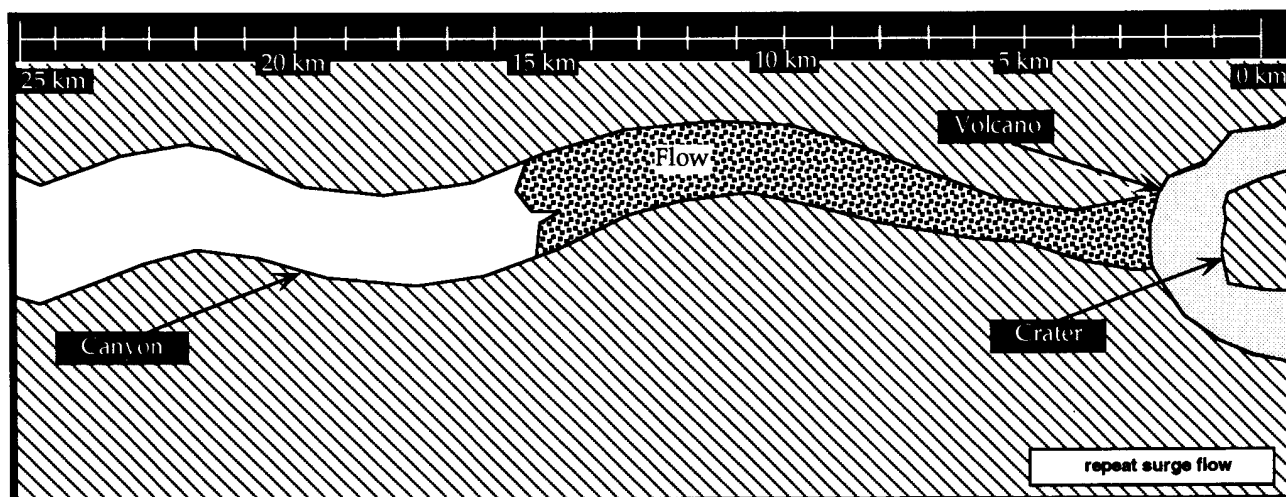


Figure 7. The graphical display of the flow consists of a separate window in which a flow can be seen to move down a canyon from a volcanic crater. Students can measure flow length directly using the scale bar at the top of the window.

Because the graphical programming environment performs numerical calculations slowly, numerical tasks can be passed to an XCMD (X-Command), which is a separate executable program that has been compiled from a high-level programming language, such as C or FORTRAN. Once the XCMD has performed the calculation, the answers are sent back to the graphical window for plotting.

The graphical display of the flow consists of a schematic aerial view of a volcano and one of its flanks (Figure 7). Because of space requirements, this display is done on a card separate from that which serves as the graphic user interface (GUI) for the calculations. The students see the flow that they have "made" by choosing values for the adjustable variables and parameters. Not only are flow lengths displayed, but flow speeds are also shown at the correct relative values.

To extract useful information from the numerical experiments, students are asked to explore the parameter space made available to them, to see which flows go fastest and which farthest, as a function of flow type and parameter values. Their results are tabulated, because they then are asked to use the results to construct a map showing the potential for hazards from the different types of eruptions. In constructing this map, the students must organize the results for the different flow phenomena according to both flow extent (length) and flow violence (velocity). Within a preconstructed graphical mapping area, students then draw in the zones in which the different flow phenomena are expected to occur, thus constructing a volcanic-hazards map, which in many

ways resembles those that are typically made by volcanologists for potentially dangerous volcanoes.

CONCLUSIONS

The examples that were discussed illustrate how a truly interactive computer system can enhance the understanding of physical laws in introductory geology and environmental courses. The primary interactive tool is an interactive graphic module that displays the solutions to the equations immediately in two or three dimensions. We find that the complex geological concepts are more readily understood and more material can be covered in a standard laboratory using these computer modules.

ACKNOWLEDGMENTS

The computer programming and development for these particular laboratories was done by Alex Schuchman, David Redmin, Mark Feldhousen (volcanoes), Rebecca Daum (earthquakes) and Elisabeth Cuddihy (mass wasting). Paul Reitan and Michael Sheridan contributed significantly to the concepts of the laboratories. The development and implementation of these laboratories in our courses has been partially supported by the National Science Foundation, Undergraduate Course and Curriculum Program (DUE9254211).

REFERENCE CITED

Jager, S., and Wiczorek, G.F., 1994, Landslide susceptibility in the Tully Valley area, Finger Lakes Region, New York: U S Geological Survey Open File Report 94-615.

Food for Thought

On a cold winter day in December 1955, Robert Wentorf, Jr. walked down to the local food co-op in Niskayuna, New York, and bought a jar of his favorite crunchy peanut butter. Back at his nearby General Electric lab he scooped out a spoonful, subjected it to crushing pressures and searing heat, and accomplished the ultimate culinary *tour de force*: he transformed the peanut butter into tiny crystals of diamond. (p. xi) . . . "The peanut butter turned into tiny green diamond crystals," Wentorf explains. "It was because of all the nitrogen" (p. 141).

Robert M. Hazen, 1993, *The new alchemists – Breaking through the barriers of high pressure*: New York, Times Books, 286 p.